Surface modification of nanocrystalline $LiCoO_2$ particles with rare earth oxides using polymeric resin process

B.Nageswara Rao[a], M.Venkateswarlu[b], N.Satyanarayana [a,*]
[a]Department of Physics, Pondicherry University, Pondicherry, 605014, INDIA
[b]R & D, Amaraja batteries, Tirupati, 517 501, AP, INDIA

ABSTRACT

Nanocrystalline $LiCoO_2$ particles were prepared using ethylene glycol assisted Pechini process and rare earth oxides (Sm_2O_3 and La_2O_3) coated nanocrystalline $LiCoO_2$ particles were prepared using newly developed polymeric resin process. The prepared particles were characterized using TG/DSC, FTIR, XRD, SEM and XRF. The electrical conductivities were evaluated through impedance measurements for the pure, Sm_2O_3 and La_2O_3 coated nanocrystalline $LiCoO_2$ particles.

Keywords: Nanocrystalline $LiCoO_2$ particles, Surface modification, XRD, FTIR, SEM, XRF, Impedance spectroscopy, Electrical Conductivity.

1.INTRODUCTION

There is a great demand for energy storage devices, such as rechargeable batteries. Among the family of rechargeable batteries, Li- ion batteries have been an increasing potential applications in portable electronic devices due to their high energy density and high specific capacity [1]. Among the available positive electrode materials, layer structured $LiCoO_2$ is the most preferred electrode used in commercial Li-ion batteries because of it's high theoretical capacity (274 $mAhg^{-1}$) [2-5]. However, $LiCoO_2$ exhibits a capacity fading at high rates due to it's structural instability and reactivity with electrolyte. During charge and discharge process, $Li_{1-x}CoO_2$ undergoes a phase transition from hexagonal to monoclinic, if x value exceeds 0.5 and hence, leads to capacity fade [6]. In order to mitigate this problem, attempts have made through coating of metal oxides over $LiCoO_2$ particles [7-10]. The coating reduces the direct contact with electrolyte and protects the original structure during charging/discharging process. In the present work, newly developed polymeric resin process was used for coating of rare earth oxides (Sm_2O_3, La_2O_3) over $LiCoO_2$ nanoparticles. The prepared rare earth oxides (Sm_2O_3, La_2O_3) coated $LiCoO_2$ powders were characterized using TG/DSC, FTIR, XRD, SEM and XRF techniques. The electrical conductivities were evaluated through impedance measurements for pure,Sm_2O_3 and La_2O_3 coated nanocrystalline $LiCoO_2$ particles.

2. EXPERIMENTAL

$LiNO_3$(s.d fine), $Co(NO_3)_2.6H_2O$ (Qualigens), citric acid anhydrous (Qualigens) and ethylene glycol (merck chemicals) were used for the synthesis of nanocrystalline $LiCoO_2$ particles by Pechini process. Required quantities of metal nitrate, citric acid and ethylene glycol solutions were prepared separately and mixed by keeping total metal ion to citric acid and ethylene glycol ratio as 1 : 1 : 1 under stirring condition. The mixed solution was evaporated at 80^0C to remove excess water. After 6-8 hours, it has turned into viscous resin. Further, the resin was heated at 150^0C for 12 hours to obtain the polymeric intermediate. The polymeric intermediate was grounded and calcined at 500^0C for 12 hours to obtain $LiCoO_2$ nanoparticles.

For Sm_2O_3 and La_2O_3 coating over $LiCoO_2$ particles, polyacrylic acid (LR grade, National chemicals), ethylene glycol (merck), samarium nitrate (AR grade, CDH), lanthanum nitrate (SRL chemicals,) and nanocrystalline $LiCoO_2$ particles were used. The required quantity of $LiCoO_2$ particles were dispersed in acetone and sonicated for 30 minutes to remove the agglomerations and then acetone was removed by drying in hot air oven. The obtained dried $LiCoO_2$ particles were dispersed in ethanol through sonication (A). The 10 : 2 molar ratio of polyacrylic acid and ethylene glycol solutions were mixed under constant stirring. The obtained clear solution was evaporated at 80^0C to remove excess water. Stoichiometric amounts of samarium nitrate / lanthanum nitrate solution was added to the PAA and EG solution under constant stirring to maintain the molar ratio of total metal ions to PAA and EG as 1 : 10 : 2. Further evaporation, leads to the formation of polymeric resin (B). A and B were mixed under vigorous stirring and the evaporation was continued for 6 hours. Finally, black coloured solid mass was obtained and was calcined at 500^0C for 6 hours to obtain Sm_2O_3 / La_2O_3 coated $LiCoO_2$ nanoparticles.

TG/DSC curves of the polymeric resins of Sm_2O_3 and La_2O_3 coated nanocrystalline $LiCoO_2$ samples were recorded at the heating rate of

Cleantech 2012, www.ct-si.org, ISBN 978-1-4665-6277-6

10^0C for minute between 30^0C and 600^0C using TA instrument SDT Q600 V20.5. FTIR spectra were recorded using shimadzu FTIR-8000 spectrometer. Powder X-ray diffraction patterns were recorded using X'pert PRO MPD, PANalytical (Philips) X-ray powder diffractometer with Cu Kα radiation of wavelength 1.54 A^0 at a scan rate of 2^0 per minute. The microstructures of all the prepared samples were imaged using scanning electron microscope (Hitachi, S-3400N model). The percentage of elements present in the samples were examined using X-ray fluorescence spectrometry (Bruker S4 Pioneer model). The impedance data of all the prepared samples were recorded using Novacontrol Alpha A high performance frequency analyzer.

3. RESULTS AND DISCUSSION

3.1. TG / DSC

TG/DSC curves of Sm_2O_3 and La_2O_3 polymeric resins coated $LiCoO_2$ nanoparticles are shown in fig.1 a, b. From fig.1a, the observed weight loss about 1.3% in TG curve between 30^0C and 130^0C is due to the removal of adsorbed moisture and the weight loss about 2 % between 170^0C and 435^0C is due to the decomposition of organic derivatives as well as removal of nitrates. The respective exothermic peaks were observed in DSC curve. TG curve does not show any more weight loss above 500^0C, which indicates the complete removal of volatiles, nitrates and organic derivatives from the polymeric resin.

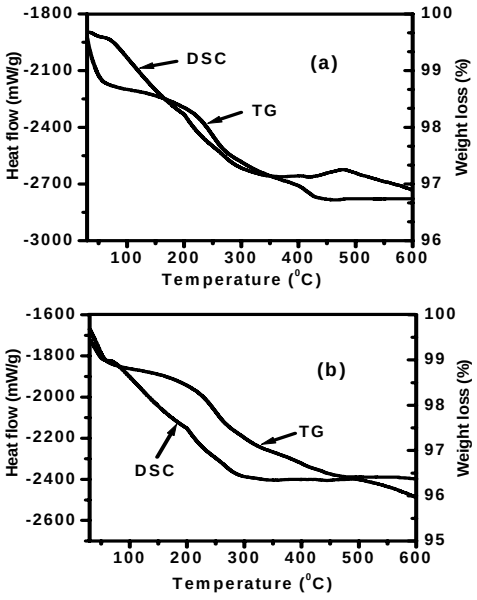

Fig.1 TG/DSC curves of a) Sm_2O_3 and b) La_2O_3 coated $LiCoO_2$ polymeric resins.

From fig.1 b, the weight loss about 1.2 % between 30^0C and 130^0C is due to the removal of adsorbed moisture and the respective endothermic peak was observed in DSC curve. The weight loss about 2.3 % between 150^0C and 465^0C with two exothermic peaks in DSC curve indicates the decomposition of organic derivatives as well as removal of nitrates.

3.2 FTIR

FTIR spectra of bare, resin, Sm_2O_3 and La_2O_3 coated $LiCoO_2$ nanoparticles are shown in fig.2 a,b. From fig.2 a, b, bare $LiCoO_2$ exhibited three peaks at 510 cm^{-1}, 550-560 cm^{-1} and 580-610 cm^{-1} and correspond to the asymmetric stretching modes of $[CoO_6]$ octahedra in $LiCoO_2$ [11]. For resin coated $LiCoO_2$, the observed IR peaks at 1577 cm^{-1} and 1475 cm^{-1} correspond to the asymmetric stretching modes of COO- groups. The sharp IR peak at 1384 cm^{-1} corresponds to NO_3^- ions [12-13]. The band between 1020-1220 cm^{-1} is due to the stretching vibration of C-O-C groups [14].

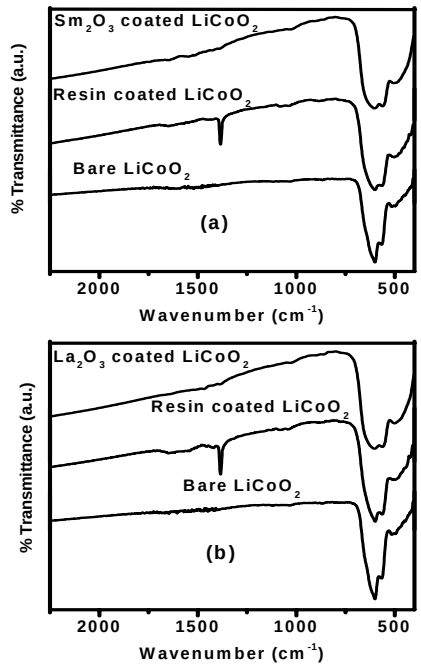

Fig.2 FTIR spectra of a) bare and resin, Sm_2O_3 coated $LiCoO_2$ and b) bare and resin, La_2O_3 coated $LiCoO_2$ particles.

For Sm_2O_3 coated $LiCoO_2$, the observed IR peaks at 530 cm^{-1} and 610 cm^{-1} attributed to the stretching modes of Sm_2O_3 structure and the shifting and broadening of the peaks at 550-560 cm^{-1} and 580-610 cm^{-1} are due to the formation of Sm_2O_3 coated $LiCoO_2$ structure. For La_2O_3 coated $LiCoO_2$, the observed peaks at 450 cm^{-1} and 640 cm^{-1} assigned to the stretching mode of La-O from La_2O_3 structure [15].The shifting and broadening of the band at 580-610 cm^{-1} may be due to the formation of La_2O_3 coated $LiCoO_2$ structure.

3.3 XRD

The XRD patterns of bare, resin, Sm_2O_3 and La_2O_3 coated $LiCoO_2$ nanoparticles are shown in fig.4a,b. From fig.3 a,b, the XRD patterns of the polymeric resin, Sm_2O_3 and La_2O_3 coated $LiCoO_2$ particles did not exhibit any extra new peaks corresponding to Sm_2O_3 and La_2O_3 phases, which indicates that the coating may be in an amorphous phase. Also, XRD patterns of bare, Sm_2O_3 and La_2O_3 coated $LiCoO_2$ nanoparticles indicate that coating of oxides did not effect the crystalline phase of the $LiCoO_2$ nanoparticles, which is confirmed by comparing the observed XRD peaks with standard JCPDS data.

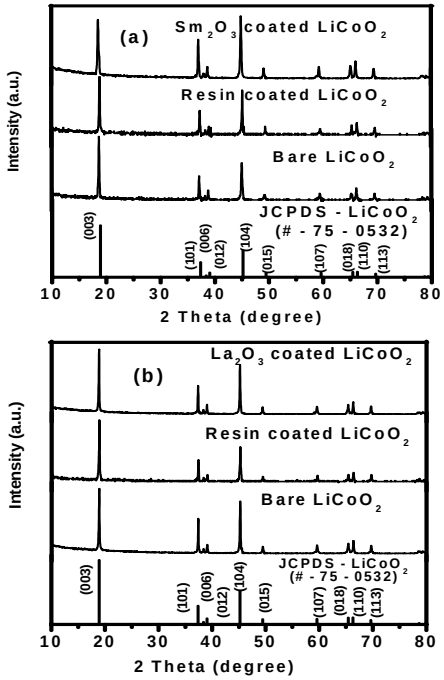

Fig.3 XRD patterns of a) bare, Sm_2O_3 polymeric resin and Sm_2O_3 coated $LiCoO_2$ and b) bare, La_2O_3 polymeric resin and La_2O_3 coated $LiCoO_2$ particles.

3.4 SEM

SEM micrographs of Sm_2O_3 and La_2O_3 coated $LiCoO_2$ nanoparticles at different magnifications are shown in fig.4a-d.Fig.4 a-b, show the SEM images of the Sm_2O_3 coated $LiCoO_2$ particles. Fig.4 c-d, show the SEM images of La_2O_3 coated $LiCoO_2$ particles. All images show a very thin nano size layer over the agglomerated $LiCoO_2$ nanoparticles, which may be due to Sm_2O_3 and La_2O_3 coating over the agglomerated $LiCoO_2$ nanoparticles.

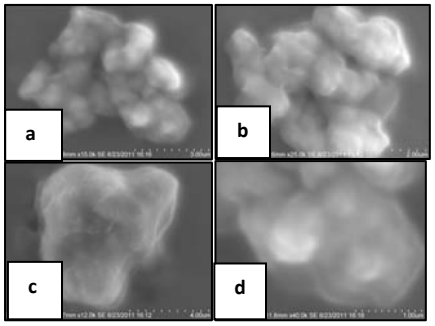

Fig.4 SEM micrographs of Sm_2O_3 coated $LiCoO_2$ (a,b) and La_2O_3 coated $LiCoO_2$ particles (c,d).

Further, presence of Sm_2O_3 and La_2O_3 in Sm_2O_3 and La_2O_3 coated $LiCoO_2$ nanoparticles are confirmed from the elemental analysis of the measured XRF spectra.

3.5. XRF

XRF spectra of Sm_2O_3 and La_2O_3 coated $LiCoO_2$ nanoparticles are shown in fig. 5a,b. From fig.5a,b, the presence of Sm_2O_3, La_2O_3 and CoO in Sm_2O_3 and La_2O_3 coated $LiCoO_2$ particles are confirmed from the observed characteristic peaks.

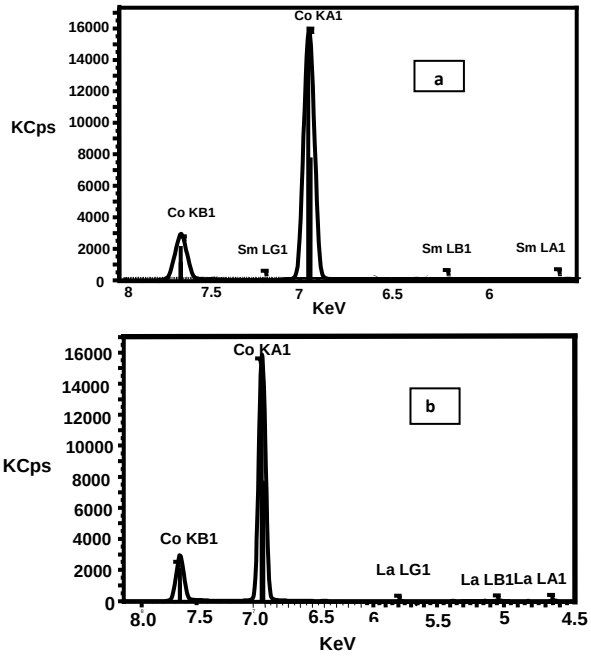

Fig.5 XRF spectra of a) Sm_2O_3 coated $LiCoO_2$ and b) La_2O_3 coated $LiCoO_2$ particles.

Lithium is not detected, since it is a light element. So, excluding the percentages of Sm_2O_3, La_2O_3 and CoO, the remaining percentage corresponds to the presence of Li_2O. The Sm_2O_3, La_2O_3 and CoO percentages are given in the table 1. Hence, XRF results confirm the presence of Sm_2O_3, La_2O_3 and CoO in Sm_2O_3 and La_2O_3 coated $LiCoO_2$ nanoparticles.

Material	CoO	Sm_2O_3	La_2O_3
Sm_2O_3 coated $LiCoO_2$	83.930	1.849	
La_2O_3 coated $LiCoO_2$	84.980		1.810

Table 2. Percentages of CoO, Sm_2O_3 and La_2O_3 exist in Sm_2O_3 and La_2O_3 coated $LiCoO_2$ nanoparticles.

3.6. Electrical Conductivity Studies

Fig.6 shows the impedance plots of bare, Sm_2O_3 and La_2O_3 coated $LiCoO_2$ nanoparticles. From fig.6, the observed two overlapped semicircles were analyzed using win fit software. The first and second semi circles indicate the grain interior and grain boundary effects respectively [16]. The grain interior (R_{gi}) and the grain boundary (R_{gb}) resistances of bare, Sm_2O_3 and La_2O_3 coated $LiCoO_2$ sample pellets sintered at 200^0C for half an hour are obtained respectively from the intercepts of first and second semicircles with the real axis. The evaluated electrical conductivities of bare, Sm_2O_3 and La_2O_3

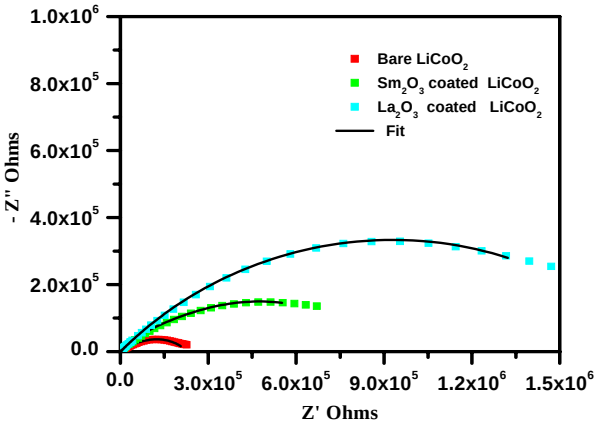

Fig.6 Impedance (Z' and -Z'') plots of bare, Sm_2O_3 and La_2O_3 coated nanocrystalline $LiCoO_2$ particles.

coated LiCoO2 particles are found to be 6.597 X 10^{-6} ohm^{-1} cm^{-1}, 4.766 X 10^{-6} ohm^{-1} cm^{-1} and 4.336 X 10^{-6} ohm^{-1} cm^{-1} respectively. It is observed that the conductivities of Sm_2O_3 and La_2O_3 coated $LiCoO_2$ particles are less compared to bare $LiCoO_2$, which may be due to the presence of nanosize Sm_2O_3 and La_2O_3 layers over the $LiCoO_2$ particles. The nano size Sm_2O_3 and La_2O_3 layers protect the $LiCoO_2$ structure during charge/discharge, which may enhance the capacity retention.

4. CONCLUSION

Nanocrystalline $LiCoO_2$ and Sm_2O_3, La_2O_3 coated $LiCoO_2$ particles were synthesized using Pechini and novel polymeric resin processes respectively. Formation of $[CoO_6]$, Sm_2O_3 and La-O of La_2O_3 structures are confirmed from FTIR spectral results. The amorphous nature of the Sm_2O_3 and La_2O_3 layers over $LiCoO_2$ particles are confirmed from the observed XRD results. The presence of Sm_2O_3, La_2O_3 and CoO are confirmed from XRF results. The Sm_2O_3 and La_2O_3 coated $LiCoO_2$ particles are found to have less conductivity, compared to bare $LiCoO_2$ particles.

Acknowledgement: NS is grateful to AICTE, Govt. of INDIA for providing financial support in the form of research project sanction No.:8023/BOR/RID/ RPS-174/ 2009-10,dated 31-03- 2010

Corresponding author: **Tel. 0413-2654404, Fax:0413-2655348,Email:nallanis2011@gmail.com**

REFERENCES

(1) Nazri, A.; Pistoia, G. Lithium batteries: Science and technology, Kluwer: Boston, 2004; p 1.
[2] L.D. Dyer, B.S. Borie Jr., G.P. Smith, J. Am. Chem. Soc. 76 (1954)1499.
[3] J.M. Tarascon, M. Armand, Nature (London) 414 (2001) 359.
[4] C. Julien, S. Gastro-Garcia, J. Power Sources 97–98 (2001) 290.
[5] M. Winter, J.O. Besenhard, M.E. Spahr, P. Nov´ak, Adv. Mater. 10 (1998)725.
[6] J. Cho, Y.J. Kim, T.J. Kim, B. Park, Angew. Chem. Int. Ed. 40 (2001)3367.
[7] Y. J. Kim, H. Kim, B. Kim, D. Ahn, J. G. Lee, T. J. Kim, D. Son,J. Cho,Y, W. Kim, and B. Park, Chem. Mater. 15 (2003) 1505.
[8] S. Oh, J. K. Lee, D. Byuna, W. I. Cho, and B. W. Cho, J. Power sources, 132 (2004) 249.
[9] B. Kim, J. G. Lee, M. Choi, J. Cho, and B. Park, J. Power sources, 126 (2004) 190.
[10] J. Kim, M. Noh, J. Cho, H. Kim, and K. B. Kim, J. Electrochem. Soc. 152 (2005) A1142.
[11]R.Ganesan, S. Vivekanandhan, T. Gnanasekaran, G. Periaswami, and R. S. Srinivasa,J.Nucl. mate. 325 (2004) 134.
[12] G. Socrates, Infrared and Raman Characteristic Group Frequencies, John Wiley and Sons, New York (2001).
[13] Y. M. Hon, K. Z. Fung, S. P. Lin, and M. H. Hon,J.Solid state Chem. 163 (2002) 231.
[14] K. J. Rao, H. B. Moudden, B. Desbat, P. Vinatier, and A. Levasseur,J.Solid State Chem.165 (2002) 42.
[15] R. A. El-mallawany, Infrared phys. 29 (1989) 781.
[16] C. Tian, Siu-Wai Chan, Solid State Ionics 134 (2000) 89.